論文内容の要旨

論文題目　**High Mobility Electrons and Two-Dimensional Superconductivity in $SrTiO_3$ Heterostructures**

（$SrTiO_3$ヘテロ構造における高移動度二次元超伝導相の創成）

氏名　小塚　裕介

I. Introduction

$SrTiO_3$ is currently widely used in oxide electronics mainly as a substrate because of the availability of atomically smooth surfaces with clear steps and terraces. Recently, there have been many efforts to realize low-dimensional electronic states in electron-doped $SrTiO_3$ in analogy to high-mobility GaAs heterostructures. Different from carriers in such conventional semiconductors, the carriers of $SrTiO_3$ originate from three highly anisotropic t_{2g} bands of titanium *d*-orbitals. Furthermore, the most outstanding feature of $SrTiO_3$ is the low-density superconductivity, where electron mobility is still high enough to observe quantum conduction. $SrTiO_3$ may be the best candidate to realize coexistence of such multiple novel quantum phenomena. Although there are only theoretical studies about the interplay between such states, it is a great challenge to make a foundation to investigate unexplored physics in real materials systems.

In this study, we aimed at fabricating superconducting low-dimensional electronic states using $SrTiO_3$. While most studies rely on the conduction at the surface of $SrTiO_3$ by forming an $LaAlO_3/SrTiO_3$ interface or using electrostatic field-effect gating, we tried to embed the conduction layer into the host insulating $SrTiO_3$. This is because the high electron mobility in $SrTiO_3$ is a result of effective screening from impurities or defects by the extremely large permittivity exceeding 10,000, and such screening may not be effective at the surface due to discontinuity of the crystal lattice.

II. Experimental

For the fabrication of thin films, we employed pulsed laser deposition using a vacuum chamber equipped with an infrared laser heating system. A $SrTiO_3$ substrate was ultrasonically washed in acetone and methanol, and mounted on a substrate holder with Pt paste for thermal contact. Thin films were deposited using Nb- or La-doped $SrTiO_3$ targets under an oxygen partial pressure as low as 10^{-8} Torr. For ablating the targets, a KrF excimer laser was used with an energy of 20 mJ/pulse (0.5 J/cm^2) and a repetition rate of 5 Hz. After growth, samples are annealed *ex-situ* at 600 °C in 1 bar flowing oxygen or *in-situ* at 900 °C under 10^{-2} Torr in order to fill oxygen vacancies introduced in the substrate as well as in the thin film. By measuring transport properties, we confirmed that oxygen vacancies are sufficiently filled

in either annealing condition.

The structure of the thin films was characterized by x-ray diffraction and atomic force microscopy, and the thickness was measured by a stylus profiler. For transport measurements, electrodes were made by direct ultrasonic bonding with Al wires onto the surface of the samples. Transport properties were measured in a cryogenic dewar equipped with a superconducting magnet. For ultra-low temperature measurements, we used a dilution refrigerator equipped with a rotator as well as 14 T superconducting magnet.

III. Results and discussions

1. Fabrication of high-quality electron-doped $SrTiO_3$ thin films

In order to realize the low-dimensional structure discussed in the Introduction section, a technique to fabricate sufficiently high-quality thin films is crucial. However, the quality of $SrTiO_3$ thin films is usually degraded compared with that of bulk single crystals, showing low electron mobility and deactivation of carriers. This is primarily because of the high density of cation defects introduced by the nonequilibrium growth process during crystallization of adatoms. This problem is solved by using high growth temperature to provide enough energy for the adatoms to migrate on the surface.

In order to investigate the growth temperature dependence of the film quality, we grew 100 nm-thick 0.1 at. % Nb-doped $SrTiO_3$ on $SrTiO_3$ substrates and measured x-ray diffraction and Hall effect. Figure 1 shows the growth temperature dependence of the lattice expansion from the bulk value and the low-temperature electron mobility. The lattice expansion reflects the amount of cation vacancies. The figure indicates that high temperature above ~ 1050 °C is necessary to obtain high-electron mobility by reducing cation defects. For the purpose of forming two-dimensional structures, we fabricated a thin-film heterostructure with 100-nm-thick undoped $SrTiO_3$ layers above and below a 1 at. % Nb-doped $SrTiO_3$ layer. Figure 2 shows the results of transport measurements at 2 K by varying the thickness of the doped

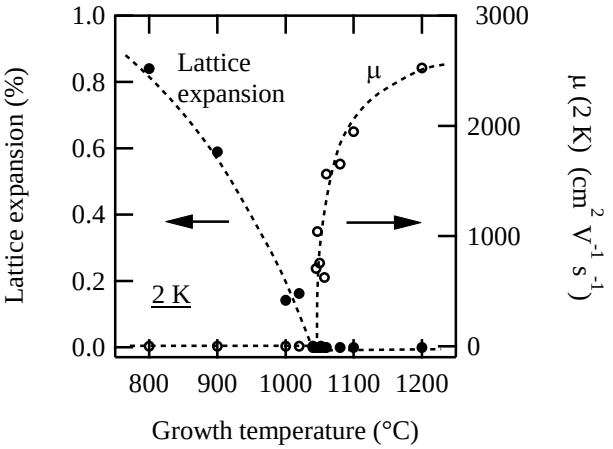

Fig. 1. Growth temperature dependence of the lattice expansion (filled circles) and electron mobility at 2 K (open circles) for 0.1 at. % Nb-doped $SrTiO_3$ grown on $SrTiO_3$ substrate. The lattice constant of bulk $SrTiO_3$ is 0.3905 nm.

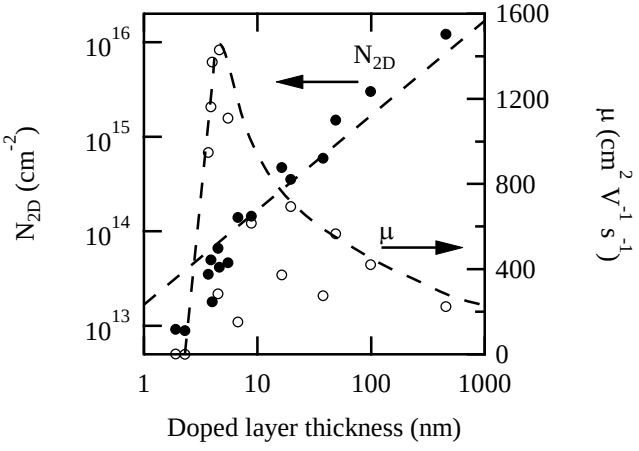

Fig. 2. Carrier density (filled circles) and electron mobility (open circles) estimated by Hall effect at 2 K as a function of doped layer thickness for the structure shown in Fig. 1. The dopant concentration of the doped layer is 1 at. %.

layer. While the carrier density is almost consistent with the nominal value, the electron mobility is enhanced by reducing the thickness of the doped layer. This may be an effect of nontrivial broadening of the electron wavefunction beyond the confined ionized impurity region.

2. Three-dimensional to two-dimensional crossover of superconductivity

Given the fabrication technique to make high-quality $SrTiO_3$ thin films, we investigated the dimensional crossover of superconductivity using the same samples as in Fig. 2. Figure 3(a) shows the temperature dependent resistivity for a sample with x = 5.5 nm, exhibiting clear superconducting transition around T = 0.37 K. Effects of dimensionality is reflected by the anisotropy of the upper critical magnetic field (H_{c2}). In two-dimensional superconductors, the temperature dependence of H_{c2} at $\theta = 0°$ and $\theta = 90°$ is expressed as $H_{c2\perp}(T) = \phi_0 / 2\pi\xi(0)^2(1-T/T_c)$ and $H_{c2\parallel}(T) = \phi_0\sqrt{12}/2\pi\xi(0)d(1-T/T_c)^{1/2}$, respectively, where ϕ_0 is the quantum flux, ξ is the coherence length, d is the superconducting thickness, and T_c is the superconducting transition temperature. The experimental data are well fitted by these equations near T_c, as shown in Fig. 3(b). The square root temperature dependence of $H_{c2\parallel}$ is characteristic of two-dimensional superconductivity in particular. By using these equations, we can estimate the superconducting thickness from $d_{\mathrm{Tinkham}} = \sqrt{6\phi_0 H_{c2\perp}/\pi H_{c2\parallel}^2}$. This value is compared with the intended thickness during thin film growth for several samples with different thickness of the conduction layer in Fig. 3(c), showing reasonable consistency in the regime $d_{\mathrm{Growth}} < \xi$.

3. Shubnikov-de Haas oscillations

Because of the enhancement of electron mobility by δ-doping in thin samples, $\omega_c\tau$ can exceed 1 at high magnetic fields, satisfying the condition to observe Shubnikov-de Haas oscillations at low

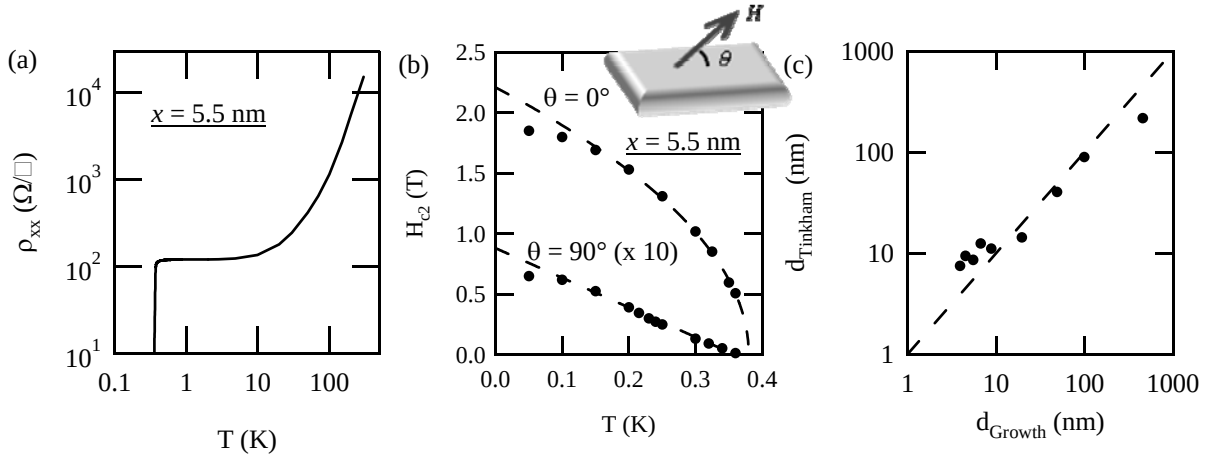

Fig. 3. Superconducting properties of a Nb-doped $SrTiO_3$ layer embedded in undoped $SrTiO_3$ layers (a) Temperature dependence of the resistivity with T_c = 0.37 K. (b) Temperature dependence of H_{c2} in the two geometries. The curves are fitting by the functional forms of $H_{c2\perp}$ and $H_{c2\parallel}$ represented in the text. The inset shows the geometry of the sample. In (a) and (b), the thickness of the conduction layer is 5.5 nm. (c) The thickness estimated using a functional form of d_{Tinkham} is compared with the intended thickness during growth.

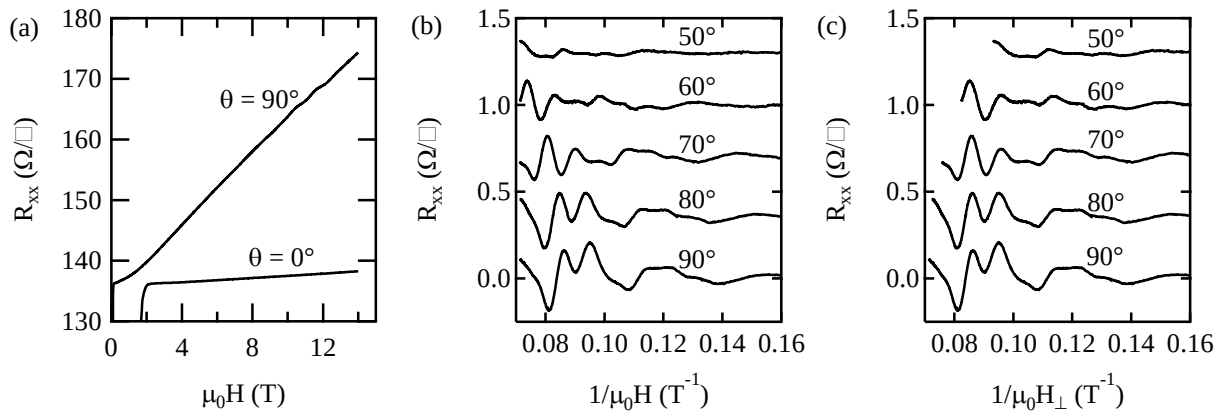

Fig. 4. (a) High-field magnetoresistance of a sample shown in Fig. 1 with x = 5.5 nm at θ = 0° and θ = 90° measured at 100 mK. (b) Angular dependence of Shubnikov-de Haas oscillations with the positive background subtracted from (a). (c) Shubnikov-de Haas oscillations plotted using $H_{\perp}=H\sin\theta$ instead of the absolute value of the magnetic field.

temperatures, where $\omega_c = eB/m^*$ is the cyclotron frequency and τ is the scattering time. High-field magnetoresistance was measured for a sample with x = 5.5 nm at 100 mK as shown in Fig. 4(a). Parallel magnetoresistance showed small magnetic-field dependence, while perpendicular magnetoresistance was strongly positive with small oscillations. By subtracting the positive background of the perpendicular magnetoresistance, clear Shubnikov-de Haas oscillations were observed, as shown in Fig 4(b). By rotating the samples with respect to the magnetic field direction, we found that the oscillations are well scaled by $H_{\perp} = H\sin\theta$ instead of the absolute value of the magnetic field, as is evident from comparing Figs. 4(b) and 4(c). This indicates a cylindrical-shaped two-dimensional Fermi surface. This is the first direct observation of a two-dimensional Fermi surface in $SrTiO_3$. However, the carrier density estimated from these oscillations is about one order of magnitude smaller than the carrier density estimated from Hall effect. This is probably because only some of the electrons in the selected subbands contribute to the oscillations, while total number of electrons are measured by Hall effect.

IV. Conclusion

In this study, we aimed at realizing a superconducting two-dimensional electron gas in $SrTiO_3$. As a result, we succeeded in making high-quality $SrTiO_3$ thin films and observing a two-dimensional Fermi surface by Shubnikov-de Haas oscillations when the thickness of the conducting layer reduced. We also observed a crossover from three-dimensional to two-dimensional superconductivity. Although multiple subband occupation prevented clear observation of a quantum Hall effect, further improvements may lead to a new phase where novel phenomena based on interplay between multiple quantum effects can be observed.